Proceedings of the 2009 IEEE International Conference on Systems, Man, and Cybernetics
San Antonio, TX, USA - October 2009

Nonlinear Robust Control to Maximize Energy Capture in a Variable Speed Wind Turbine Using an Induction Generator

Erhun Iyasere, Darren M. Dawson, John R. Wagner
College of Engineering and Science
Clemson University
Clemson, USA

Mohammed Salah
Department of Mechatronics Engineering
Hashemite University
Zarqa, Jordan

Enver Tatlicioglu
Department of Electrical and Electronics Engineering,
Izmir Institute of Technology
Urla, Turkey

Abstract—The emergence of wind turbine systems for electric power generation can help satisfy the growing global demand. This paper proposes a control strategy to maximize the wind energy captured in a variable speed wind turbine, with an internal induction generator, at low to medium wind speeds. The proposed strategy controls the tip speed ratio, via the rotor angular speed, to an optimum point at which the efficiency constant (or power coefficient) is maximal for a particular blade pitch angle and wind speed. This control method allows for aerodynamic rotor power maximization without exact wind turbine model knowledge.

Key Words—Induction generators, robustness, torque control, wind power generation

NOMENCLATURE

β	Blade pitch angle (rad).
C_p	Power capture efficiency.
I	Current (A).
L	Inductance (H).
λ	Tip speed ratio.
M	Mutual inductance (H).
M_m	Moment of inertia (kg.m^2).
n_p	Number of generator pole pairs.
ω	Rotor angular velocity (rad/s).
$\bar{\Psi}, \Psi$	Flux Linkage (Wb).
P	Power (W).
R	Resistance (Ω).
R_a	Blade radius.
ρ_a	Air density (kg/m^3).
τ_{em}	Electromagnetic torque (N.m).
v	Wind velocity (m/s^2)
V_r	Rotor Voltage (V)

Subscripts and Superscripts

*	Optimal value
a, b	Fixed stator frame component
d	Desired value
L	Load
max	Maximum value
r, s	Rotor, stator

I. INTRODUCTION

Wind energy has evolved into an attractive energy source for electric utilities, it is currently responsible for about one percent of the global electrical power production. The structure of wind turbines, as well as the fact that the wind energy rate is uncontrollable, complicates the problem of regulating the power capture. This engineering challenge has been alleviated by the construction of variable speed wind turbines, which are designed to regulate the power captured over a range of operating speeds. However, the efficiency of power regulation is dependent on the selected control method.

The standard region 2 (power capture maximization mode) control scheme used for variable speed wind turbines, ($\tau = k\omega^2$, where τ is the control torque, ω is the rotor angular speed and k is a control gain), has some disadvantages that can result in unsatisfactory power capture. First, the control gain k is difficult to determine due to the dependence on exact model knowledge (maximum power efficiency constant and optimal tip speed ratio). Secondly, the standard value of k might not provide the maximum energy capture under real world turbulent conditions. Johnson and Fingersh [1] showed via simulation that smaller values of k than the standard can result in increased power capture. They proposed a new control scheme: an adaptive control scheme that allows for maximum power capture in presence of parameter uncertainty. Similar adaptive control techniques for wind turbine control were developed in [2] and [3].

Other wind turbine control methods like classical control techniques [4]-[7], robust control [8] and fuzzy logic control [9]-[10] have been utilized to regulate rotor speed, regulate pitch angle and to enhance energy capture. Iyasere et al. [8] proposed a robust control strategy to control the blade pitch angle and rotor speed in a variable speed, variable pitch wind turbine in order to maximize the energy capture, without the knowledge of the optimal tip speed ratio and in the presence of model structural uncertainties.

An area of particular importance is the control of the internal generators used in wind turbines. The most commonly used generator is the induction generator; the types of which include cage, wound rotor and doubly fed induction generator (DFIG). The dynamic modeling [11]-[15] and control [16]-[23] of induction machines has been extensively researched. Thringer and Luomi [11] examined the validity of various dynamic models of induction machines to include the fifth-order Park model and other reduced order models by predicting the low frequency dynamic response of a 15 kW induction machine and comparing results to actual measurements. They concluded that the Park model accurately predicts rotor speed, electrical torque, active power, reactive power and stator current responses to perturbations in the shaft torque, supply frequency and voltage magnitude. In power system analysis, a third order model was determined to be the right fit of accuracy and simplicity. Tapia et al. [12] developed the mathematical model of a grid connected wind driven DFIG and presented a comparison of the simulation results to real machine performance results. They also developed a stator-flux-oriented vector control based technique to control the generator power factor. Mullane and O'Malley [13] examined the inertial response of a squirrel cage and a doubly fed induction wind turbine generator using fifth-order induction generator models. They discovered that a DFIG utilizing field-oriented control is strongly influenced by rotor current controller bandwidth. Hu and Dawson [16] presented an adaptive partial state feedback position tracking controller for the full-order nonlinear dynamic model for an induction motor. The controller compensates for uncertainty in rotor resistance and mechanical system parameters while yielding asymptotic rotor position tracking. Pena et al. [18] describes a vector control scheme for the supply-side voltage source-converter of a DFIG for independent control of active and reactive power. This strategy was embedded into an optimal tracking controller in order to maximize energy capture in a wind energy application.

In this study, a control strategy is developed to regulate the rotor speed of a small variable speed wind turbine system with an induction generator. The control objective is to maximize the energy captured by the wind turbine for low to medium air speeds by tracking a desired rotor speed in the presence of system nonlinearities and structural uncertainty. Additionally, the maximization of the energy captured is achieved without the knowledge of the relationship that governs the power capture efficiency of the wind turbine. Instead, an optimization algorithm is developed to seek the unknown optimal rotor speed that maximizes the energy captured (via the aerodynamic rotor power), at a particular blade pitch angle and wind speed, while ensuring that the resulting trajectory is sufficiently differentiable. The disadvabtage of not explicitly knowing the rotor speed *a priori* is countered by the fact that the optimal rotor speed will change as the wind speed changes which may be accommodated for by choosing the right optimization algorithm. A robust controller is designed and proven to yield a globally uniformly ultimately bounded (GUUB) stable closed loop system through Lyapunov-based analysis.

The paper is organized as follows. In Section II, the system model and problem statement are mathematically formulated. In Section III, a robust speed tracking controller is designed and the stability analysis is presented. In Section IV, an observer is designed to estimate the system nonlinearities. In Section V, the estimate of the system nonlinearities is used to generate the rotor speed reference trajectory. Concluding remarks are presented in Section VI.

II. System Model

The wind turbine model consists of a wind rotor, drive shaft and an internal induction generator. The system block diagram is shown in Fig. 1. The aerodynamic rotor power captured by the wind turbine is dependent on the available wind power and the power coefficient, C_p, which is a function of the tip-speed ratio (TSR) $\lambda(t)\in\mathbb{R}$, and the blade pitch angle, $\beta\in\mathbb{R}$. The rotor power of the wind turbine, $P_{\text{aero}}(t)\in\mathbb{R}$, can be defined as

$$P_{\text{aero}}=\frac{1}{2}C_p\rho_a\pi R_a{}^2v^3 \tag{1}$$

where $C_p(\lambda,\beta)\in\mathbb{R}$ is assumed to be unknown. The tip-speed ratio, $\lambda(t)$, is defined as

$$\lambda=\frac{\omega R_a}{v}. \tag{2}$$

From (1) and (2), it can be inferred that there exists a constant optimal rotor speed, ω^*, for a particular wind speed, $v(t)$, and blade pitch angle, β, at which the power capture efficiency, and thus the aerodynamic rotor power is

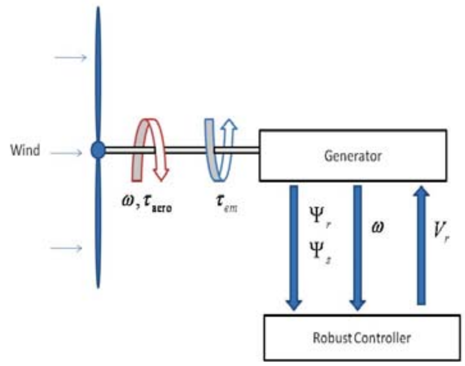

Figure 1. Block diagram of wind turbine system

maximum, with $P_{\max} \triangleq \frac{1}{2} C_p^{\max} \rho_a \pi R_a^2 v^3$, $C_p^{\max} = C_p(\lambda^*, \beta)$ and $\lambda^* = \frac{\omega^* R_a}{v}$ [1].

The rotor power, $P_{aero}(t)$, can also be written as

$$P_{aero} = \tau_{aero}\omega \tag{3}$$

where $\tau_{aero}(t) \in \mathbb{R}$ is the aerodynamic torque applied to the rotor by the wind. An expression for $\tau_{aero}(t)$ can be derived from (1)-(3) as

$$\tau_{aero} = \frac{1}{2} \rho_a \pi R_a^3 \frac{C_p}{\lambda} v^2. \tag{4}$$

Remark 1.1: In (1), it is assumed that $C_p(\cdot)$ is unknown which implies that $\tau_{aero}(t)$ and $P_{aero}(t)$ are unmeasurable.

A. Mechanical Subsystem Dynamics

The mechanical subsystem describes the rotor dynamics of the variable speed wind turbine and is assumed to be of the form

$$M_m \dot{\omega} + f = \tau_{em} \tag{5}$$

where $\dot{\omega}(t)$ is the rotor acceleration, and $f(\omega, v) \triangleq -\tau_{aero}(t)$ represents the system nonlinearities.

B. Electrical Subsystem Dynamics

The standard induction machine model can be found in [24]. The model utilized in this paper is the transformed nonlinear induction machine model in the stator fixed *a-b* reference frame with the assumptions of equal mutual and auto inductances, and a linear magnetic circuit [19]. The electrical dynamics of the internal induction generator can be described by the following dynamic equations:

$$\dot{\bar{\Psi}}_s = -(R_s + R_L)\bar{I}_s \tag{6}$$

$$\dot{\bar{\Psi}}_r = -R_r \bar{I}_r + n_p \omega J \bar{\Psi}_r + \bar{V}_r \tag{7}$$

$$\bar{I}_s = \kappa_1 \bar{\Psi}_s - \kappa_2 \bar{\Psi}_r \tag{8}$$

$$\bar{I}_r = \kappa_1 \bar{\Psi}_r - \kappa_2 \bar{\Psi}_s \tag{9}$$

$$\tau_{em} = \alpha \bar{\Psi}_s^T J \bar{\Psi}_r \tag{10}$$

$$J = \begin{bmatrix} 0 & -1 \\ 1 & 0 \end{bmatrix}, \quad \alpha = n_p \kappa_2 \tag{11}$$

where $\bar{\Psi}_s = \left[\bar{\Psi}_{s_a}, \bar{\Psi}_{s_b}\right]^{\mathrm{T}}$, $\bar{\Psi}_r = \left[\bar{\Psi}_{r_a}, \bar{\Psi}_{r_b}\right]^{\mathrm{T}}$, $\bar{V}_r = \left[\bar{V}_{r_a}, \bar{V}_{r_b}\right]^{\mathrm{T}}$, $\bar{I}_s = \left[\bar{I}_{s_a}, \bar{I}_{s_b}\right]^{\mathrm{T}}$, $\bar{I}_r = \left[\bar{I}_{r_a}, \bar{I}_{r_b}\right]^{\mathrm{T}} \in \mathbb{R}^2$. In (8) and (9), κ_1 and κ_2 are constants related to the motor parameters, and are given explicitly by

$$\kappa_1 = \frac{L_s}{L_s^2 - M^2}, \quad \kappa_2 = \frac{M}{L_s^2 - M^2} \tag{12}$$

To facilitate control development, the following model characteristics are assumed:

Assumption 1: The parameters L_s, M, M_m, n_p, R, R_L, R_r, R_s, β and ρ_a are known constants.

Assumption 2: $\omega(t)$, $\bar{I}_s(t)$, $\bar{I}_r(t)$, and $v(t)$ are measurable.

Assumption 3: $v(t)$ is constant or slowly time varying (*i.e.*, $\dot{v} \cong 0$).

Assumption 4: $v(t), \dot{v}(t), \ddot{v}(t)$ are bounded.

Assumption 5: As a consequence of the fact that $\tau_{aero}(t)$ is unknown, $f(\omega, v)$, introduced in (5) is also unknown .

Assumption 6: The variables, $f(\cdot)$, $\dot{f}(\cdot)$, $\ddot{f}(\cdot)$ are bounded provided that $\omega(t)$, $\dot{\omega}(t)$, $\ddot{\omega}(t)$ are bounded.

Remark 2.1: $f(\omega, v)$ can be upper bounded by a known function such that $|f(\omega, v)| \le \rho(\omega)$ where $\rho(\omega)$ is continuously differentiable for all $\omega(t) > 0$.

C. Electrical Subsystem Transformation

An auxiliary control input $\omega_s(t)$ is injected into the electrical subsystem dynamics via time-varying coordinate transformation [20] as follows

$$\Psi_s \triangleq T\bar{\Psi}_s, \quad I_s \triangleq T\bar{I}_s \quad V_r \triangleq T\bar{V}_r \\ \Psi_r \triangleq T\bar{\Psi}_r, \quad I_r \triangleq T\bar{I}_r \tag{13}$$

where $T(t) \in \mathbb{R}^{2\times 2}$ is defined as

$$T \triangleq \begin{bmatrix} \cos(\varepsilon_0) & \sin(\varepsilon_0) \\ -\sin(\varepsilon_0) & \cos(\varepsilon_0) \end{bmatrix} \tag{14}$$

where $\dot{\varepsilon}_0 = \omega_s$. It should be noted that $T(t)$ satisfies $T^{-T} J T^{-1} = J$.

The overall dynamics of the induction generator can then be given by the following fifth order model:

$$M_m \dot{\omega} + f = \tau_{em} \tag{15}$$

$$\dot{\Psi}_s = -R_o \kappa_1 \Psi_s + R_o \kappa_2 \Psi_r - J \Psi_s \omega_s \tag{16}$$

$$\dot{\Psi}_r = V_r - R_r \kappa_1 \Psi_r + R_r \kappa_2 \Psi_s + n_p \omega J \Psi_r - J \Psi_r \omega_s \tag{17}$$

$$\tau_{em} = \alpha \Psi_s^{\mathrm{T}} J \Psi_r \tag{18}$$

$$I_s = \kappa_1 \Psi_s - \kappa_2 \Psi_r \tag{19}$$

$$I_r = \kappa_1 \Psi_r - \kappa_2 \Psi_s \tag{20}$$

where $\Psi_s = \left[\Psi_{s_1}, \Psi_{s_2}\right]^{\mathrm{T}}$, $\Psi_r = \left[\Psi_{r_1}, \Psi_{r_2}\right]^{\mathrm{T}}$, $V_r = \left[V_{r_1}, V_{r_2}\right]^{\mathrm{T}}$, $R_o \triangleq R_s + R_L$.

III. Controller Design

A. Control Objective

The objective in this paper is to maximize the aerodynamic rotor power of the wind turbine, $P_{\text{aero}}(t)$, by tracking a developed desired rotor speed $\omega_d(t) \in \mathbb{R}$ such that $\omega(t) \to \omega_d(t)$ as $t \to \infty$. This is achieved in turn by tracking a desired electromagnetic torque, $\tau_d(t) \in \mathbb{R}$, a desired stator flux $\Psi_s^{\,d}(t) \in \mathbb{R}^{2\times 1}$, and a desired rotor flux $\Psi_r^{\,d}(t) \in \mathbb{R}^{2\times 1}$ such that $\Psi_s(t) \to \Psi_s^{\,d}(t)$, $\Psi_r(t) \to \Psi_r^{\,d}(t)$, and $\tau_{em}(t) \to \tau_d(t)$ as $t \to \infty$ where

$$\Psi_s^{\,d} = \left[\Psi_{s_1}^{\,d}, 0\right]^{\mathrm{T}} \quad \Psi_r^{\,d} = \left[\Psi_{r_1}^{\,d}, \Psi_{r_2}^{\,d}\right]^{\mathrm{T}} \tag{21}$$

$$\tau_d \triangleq \alpha \left(\Psi_s^{\,d}\right)^T J \Psi_r^{\,d} \tag{22}$$

Remark 3.1: The desired rotor speed, $\omega_d(t)$, is designed online using a numerical-based optimization algorithm, as shown in Section V, to maximize the rotor power $P_{\text{aero}}(t)$ at a particular blade pitch angle, β , and wind velocity, $v(t)$, such that $\omega_d(t) \to \omega^*$, where the optimal speed, ω^*, is the result of the optimum seeking algorithm after convergence, hence $P_{\text{aero}}(t) \to P_{\max}$ if $\omega(t) \to \omega_d(t)$. Additionally, $\omega_d(t)$ is designed such that $\omega_d(t), \dot{\omega}_d(t), \ddot{\omega}_d(t) \in \mathcal{L}_\infty$.

Remark 3.2: The desired rotor flux, $\Psi_{s_1}^{\,d}(t)$, is designed such that $\Psi_{s_1}^{\,d}(t) > 0$, $\Psi_{s_1}^{\,d}(t), \dot{\Psi}_{s_1}^{\,d}(t), \ddot{\Psi}_{s_1}^{\,d}(t) \in \mathcal{L}_\infty$, and power loss in the system is minimized, as shown in [25].

Remark 3.3: To ensure equality in (22), $\Psi_{r_2}^{\,d}(t)$ is designed such that $\Psi_{r_2}^{\,d} = \dfrac{-\tau_d}{\alpha \Psi_{s_1}^{\,d}}$.

B. Error System Development

To quantify the stated control objective, rotor speed, stator flux and rotor flux tracking errors denoted by $e(t) \in \mathbb{R}$, $\eta_s(t), \eta_r(t) \in \mathbb{R}^{2\times 1}$ respectively, are defined as

$$e \triangleq \omega_d - \omega \tag{23}$$

$$\eta_s = \begin{bmatrix} \eta_{s_1} \\ \eta_{s_2} \end{bmatrix} = \begin{bmatrix} \Psi_{s_1}^{\,d} \\ 0 \end{bmatrix} - \begin{bmatrix} \Psi_{s_1} \\ \Psi_{s_2} \end{bmatrix} \tag{24}$$

$$\eta_r = \begin{bmatrix} \eta_{r_1} \\ \eta_{r_2} \end{bmatrix} = \begin{bmatrix} \Psi_{r_1}^{\,d} \\ \Psi_{r_2}^{\,d} \end{bmatrix} - \begin{bmatrix} \Psi_{r_1} \\ \Psi_{r_2} \end{bmatrix} \tag{25}$$

where $\eta_{s_1}(t), \eta_{s_2}(t), \eta_{r_1}(t), \eta_{r_2}(t) \in \mathbb{R}$.

From the definition of the tracking errors in (23), and subsystem dynamics in (5), a rotor speed open loop error system is developed as follows

$$M_m \dot{e} = M_m \dot{\omega}_d + f - \tau_{em} \tag{26}$$

Substituting in (18) and adding and subtracting (22) to the right hand side of (26) results in

$$\begin{aligned} M_m \dot{e} = {} & M_m \dot{\omega}_d + f - \tau_d \\ & + \alpha \left[\left(\Psi_s^{\,d}\right)^T J \Psi_r^{\,d} - \Psi_s^{\mathrm{T}} J \Psi_r \right]. \end{aligned} \tag{27}$$

Substituting in (24) and (25) into (27), and performing simple algebraic manipulations, results in

$$\begin{aligned} M_m \dot{e} = {} & M_m \dot{\omega}_d + f - \tau_d - \alpha \Psi_{s_1}^{\,d} \eta_{r_2} + \alpha \Psi_{r_1}^{\,d} \eta_{s_2} \\ & - \alpha \Psi_{r_2}^{\,d} \eta_{s_1} - \alpha \eta_{s_2} \eta_{r_1} + \alpha \eta_{s_1} \eta_{r_2} \end{aligned}. \tag{28}$$

Similarly, the stator and rotor flux open loop error systems are developed as follows

$$\begin{bmatrix}\dot{\eta}_{s_1}\\ \dot{\eta}_{s_2}\end{bmatrix}=\begin{bmatrix}\dot{\Psi}_{s_1}{}^{d}\\ 0\end{bmatrix}+R_o\kappa_1\begin{bmatrix}\Psi_{s_1}{}^{d}\\ 0\end{bmatrix}-R_o\kappa_1\begin{bmatrix}\eta_{s_1}\\ \eta_{s_2}\end{bmatrix}+R_o\kappa_2\begin{bmatrix}\eta_{r_1}\\ \eta_{r_2}\end{bmatrix}-R_o\kappa_2\begin{bmatrix}\Psi_{r_1}{}^{d}\\ \Psi_{r_2}{}^{d}\end{bmatrix}+\begin{bmatrix}0\\ \Psi_{s_1}{}^{d}\end{bmatrix}\omega_s+\begin{bmatrix}\eta_{s_2}\\ -\eta_{s_1}\end{bmatrix}\omega_s \quad (29)$$

$$\begin{bmatrix}\dot{\eta}_{r_1}\\ \dot{\eta}_{r_2}\end{bmatrix}=\begin{bmatrix}\dot{\Psi}_{r_1}{}^{d}\\ \dot{\Psi}_{r2}{}^{d}\end{bmatrix}+R_r\kappa_2\begin{bmatrix}\eta_{s_1}\\ \eta_{s_2}\end{bmatrix}-R_r\kappa_2\begin{bmatrix}\Psi_{s_1}{}^{d}\\ 0\end{bmatrix}+R_r\kappa_1\begin{bmatrix}\Psi_{r_1}{}^{d}\\ \Psi_{r_2}{}^{d}\end{bmatrix}-R_r\kappa_1\begin{bmatrix}\eta_{r_1}\\ \eta_{r_2}\end{bmatrix}+n_p\omega\begin{bmatrix}-\eta_{r_2}\\ \eta_{r_1}\end{bmatrix}-n_p\omega\begin{bmatrix}-\Psi_{r_2}{}^{d}\\ \Psi_{r_1}{}^{d}\end{bmatrix}-\begin{bmatrix}V_{r_1}\\ V_{r_2}\end{bmatrix}+\begin{bmatrix}-\Psi_{r_2}{}^{d}\\ \Psi_{r_1}{}^{d}\end{bmatrix}\omega_s-\begin{bmatrix}-\eta_{r_2}\\ \eta_{r_1}\end{bmatrix}\omega_s \quad (30)$$

where (16), (17), and the time derivatives of (24) and (25) were utilized.

C. Control Input Design

The control inputs will be designed based on the subsequent stability analysis as well as the structure of the open loop error systems in (28)-(30).

The desired torque trajectory, $\tau_d(t)$ is designed to be

$$\tau_d = Ke+\frac{\rho^2(\omega)e}{\varepsilon}+M_m\dot{\omega}_d-\hat{f}_s \quad (31)$$

where $\hat{f}_s(\cdot)\triangleq\frac{1}{\sigma s+1}\text{sat}\{\hat{f}(\cdot)\}$, $\text{sat}\{\bullet\}$ is the saturation function, $\hat{f}(\cdot)$ is an estimate of $f(\cdot)$ designed later in Section IV, $s\in\mathbb{C}$ is the Laplace variable, $K\in\mathbb{R}^+$ is a control gain, $\varepsilon,\sigma\in\mathbb{R}^+$ are constants and $\rho(\omega)$ was previously defined in Remark 2.1.

Remark 3.4: Since $\frac{1}{\sigma s+1}$ is a proper bounded filter and the output of the saturation function is always bounded then it can be concluded that $\hat{f}_s(\cdot),\dot{\hat{f}}_s(\cdot)\in\mathcal{L}_\infty$. Thus, it may be concluded that $\left|\hat{f}_s(\cdot)\right|\le\rho_s$ where $\rho_s\in\mathbb{R}^+$.

The first entry of the desired rotor flux, $\Psi_{r_1}{}^{d}(t)$, is designed to be

$$\Psi_{r_1}{}^{d}=\frac{1}{R_o\kappa_2}\left[\dot{\Psi}_{s_1}{}^{d}+R_o\kappa_1\Psi_{s_1}{}^{d}-\alpha\Psi_{r_2}{}^{d}e-R_o\kappa_1\eta_{s_1}+\kappa_{s_1}\eta_{s_1}\right] \quad (32)$$

where $\kappa_{s_1}\in\mathbb{R}^+$ is a control gain. The auxiliary control input, $\omega_s(t)$, is designed to be

$$\omega_s=\frac{1}{\Psi_{s_1}{}^{d}}\left[R_o\kappa_2\Psi_{r_2}{}^{d}-\alpha\Psi_{r_1}{}^{d}e+R_o\kappa_1\eta_{s_2}-\kappa_{s_2}\eta_{s_2}\right] \quad (33)$$

where $\kappa_{s_2}\in\mathbb{R}^+$ is a control gain.

The control voltage, $V_r(t)$ is designed as follows

$$\begin{aligned}V_{r_1}=&\frac{\ddot{\Psi}_{s_1}{}^{d}}{R_o\kappa_2}+\Theta_1\dot{\Psi}_{s_1}{}^{d}-\Theta_2\Psi_{s_1}{}^{d}+\Theta_3\Psi_{r_1}{}^{d}+\Theta_4\Psi_{r_2}{}^{d}\\&+\left(\Theta_5-\Theta_6 e+\Theta_7 e^2\right)e+\left(\Theta_8-\Theta_9\Psi_{r_2}{}^{d}e\right)\eta_{s_1}\\&-\left(\Theta_{10}+\Theta_{11}e\right)\eta_{s2}+\left(\Theta_{12}-\Theta_9 e\right)\eta_{s_2}\eta_{r_1}+\Theta_{13}\eta_{r_1}\end{aligned} \quad (34)$$

$$\begin{aligned}V_{r_2}=&\Omega_1-\Omega_2\hat{f}_s-\Omega_3 e+\alpha e\eta_{s_1}+\Omega_4\Psi_{r_2}{}^{d}\eta_{s_1}+\Omega_5\eta_{s_2}\\&+\frac{\alpha^2\Psi_{s_1}{}^{d}\Psi_{r_2}{}^{d}}{R_o\kappa_2 M_m}\eta_{r_1}-\left(\Omega_6-\Omega_7\eta_{s_1}\right)e\eta_{r_1}\\&-\frac{\alpha^2\Psi_{r_2}{}^{d}}{R_o\kappa_2 M_m}\eta_{s_1}\eta_{r_1}+\Omega_8\eta_{s_2}\eta_{r_1}\\&-\Omega_8\eta_{s_1}\eta_{r_2}+\Omega_9\eta_{r_2}-\Omega_{10}e^2\end{aligned} \quad (35)$$

where the terms $\Theta_i(t),\Omega_j(t)$, $i=1,\ldots,13$ and $j=1,\cdots,10$, are measurable and explicitly defined in [25].

D. Analysis of tracking error systems

Theorem 1: Given the error system in (28)-(30) and the designed terms in (31)-(35), all signals are bounded and the tracking error signals given in (23)-(25) are globally uniformly ultimately bounded (GUUB).

Proof: See [25].

IV. Nonlinearity observer design

The existence of uncertain system nonlinearities in (5) motivates the design of an observer, denoted by $\hat{f}(\cdot)\in\mathbb{R}$, to estimate $f(\cdot)$. This estimate is developed for two reasons:

- $\hat{f}(\cdot)$ is used as a feed-forward term in the control design through $\hat{f}_s(\cdot)$.
- Since $P_{\text{aero}}(t)$ is unmeasurable, an estimate of the captured power, denoted by $\hat{P}_{\text{aero}}(t)\in\mathbb{R}$, is designed where $\hat{P}_{\text{aero}}(t)=-\hat{f}(t)\omega(t)$, and is used in the online planning of $\omega_d(t)$.

See [25] for design.

V. TRAJECTORY GENERATOR

In Remark 3.1, it is assumed that a desired trajectory $\omega_d(t)$ can be designed such that $\omega_d(t), \dot{\omega}_d(t)$ and $\ddot{\omega}_d(t)$ are bounded and $\omega_d(t) \rightarrow \omega^*$, where ω^* is the unknown rotor speed that maximizes the aerodynamic rotor power, $P_{\text{aero}}(t)$, for a particular wind speed, $v(t)$, and blade pitch angle, β. As stated in Remark 1.1, $P_{\text{aero}}(t)$ is unmeasurable, therefore the estimated captured power, $\hat{P}_{\text{aero}}(t)$, is used as the cost function to be optimized. The optimum seeking algorithm selected is the Successive Quadratic Estimator (SQE). The advantage of using this algorithm over conventional methods, such as the Golden Section Search, is that no initial cost function values or bounds on the functional values are required. The estimator approximates the unimodal cost function, $\hat{P}_{\text{aero}}(\hat{\omega}(t))$, as a quadratic function over a local bound and successively uses this property to predict the location of ω^*, the optimum rotor speed [26]. To ensure that $\omega_d(t), \dot{\omega}_d(t)$ and $\ddot{\omega}_d(t)$ are bounded, a filter based form of the SQE is used, wherein at each iteration (new guess), $\omega_d[n]$ is passed through a set of third order stable and proper low pass filters to generate continuous bounded signals for $\omega_d(t), \dot{\omega}_d(t)$ and $\ddot{\omega}_d(t)$.

VI. CONCLUSION

A nonlinear control strategy has been developed for a variable speed wind turbine system to optimize the energy captured by the wind turbine for a particular blade pitch angle. A desired rotor speed trajectory generator is presented that seeks the unknown optimal rotor speed while ensuring the trajectory remains bounded and sufficiently differentiable. To track the desired trajectory, a robust tracking controller is developed. The proposed controller is proven to yield a globally uniformly ultimately bounded results while keeping the closed-loop system stable via Lyapunov-based analysis. Future research will involve the implementation of the control strategy on the EXTRACTOR wind turbine and eliminating the assumption of constant or slowly time varying wind speed.

REFERENCES

[1] K. Johnson, L. Fingersh, M. Balas, and L. Pao, "Methods for increasing region 2 power capture on a variable-speed wind turbine", J. Solar Energy Eng., vol. 126, no. 4, pp. 1092-1100, 2004.

[2] U. Ozbay, E. Zergeroglu and S. Sivrioglu, "Adaptive backstepping control of variable speed wind turbines," International Journal of Control, vol. 81, no. 6, pp. 910-919, Jun. 2008.

[3] Y. Song, B. Dhinakaran, and X. Bao, "Variable speed control of wind turbines using nonlinear and adaptive algorithms," J. Wind Eng. Ind. Aerodyn., vol. 85, no. 3, pp. 293-308, Apr. 2000.

[4] M. Hand and M. Balas, "Non-linear and linear model based controller design for variable-speed wind turbines," pp. 1–8. NREL Report No. CP-500-26244.

[5] B. Liebst, "Pitch control system for large-scale wind turbines," J. of Energy, vol. 7, no. 2, pp. 182-192, 1983

[6] T. Knudsen, P. Andersen, and S. Tiffner-Clausen, "Comparing PI and robust control pitch controllers on a 400KW wind turbine by full scale tests," Department of Control Engineering, Aalborg University, Aalborg, Denmark, Tech. Rep. R-97-4174, 1997.

[7] K. Stol and M. Balas, "Full-state feedback control of a variable-speed wind turbine: A comparison of periodic and constant Gains", J. of Solar Energy Eng., vol. 123, no. 4, pp. 319-326, 2001.

[8] E. Iyasere, M. Salah, D. Dawson and J. Wagner, "Nonlinear robust control to maximize energy capture in a variable speed wind turbine", Proc. of the American Control Conference, pp. 1824-1829, Seattle, WA, Jun. 2008.

[9] R. Chedid, S. Karaki, and C. El-Chamali, "Adaptive fuzzy control for wind-diesel weak power systems," IEEE Trans. Energy Conversion, vol. 15, no. 1, pp. 71-78, Mar. 2000.

[10] X. Zhang, W. Wang and Y. Liu, "Fuzzy control of variable speed wind turbine," Proc. 6th World Congress on Intelligent Control and Automation, pp. 3872-3876, Dalian, China, 2006.

[11] T. Thiringer and J. Luomi, "Comparison of reduced-order dynamic models of induction machines," IEEE Trans. Power Syst., vol. 16, no. 1, pp. 119-126, Feb. 2001.

[12] A. Tapia, G. Tapia, J. Ostolaza, and J. Saenz, "Modeling and control of a wind turbine driven doubly fed induction generator," IEEE Trans. Energy Conversion, vol. 18, no. 2, pp. 194-204, Jun. 2003.

[13] A. Mullane and M. O'Malley, "Inertial response of induction-machine-based wind turbines" IEEE Trans. Power Syst., vol. 20, no. 3, pp. 1496-1503, Aug. 2005.

[14] J. Cathey, R. Calvin, and A. Ayoub, "Transient load model of an induction motor," IEEE Trans. Power Apparatus and Syst., vol. 92, no. 4, pp. 1399-1406, Jul. 1973.

[15] S. Muller and M Deicke "Doubly fed induction generator systems for wind turbines," IEEE Ind. Appl. Mag., pp 26-33, Jun. 2002.

[16] J. Hu and D. Dawson "Adaptive control of induction motor systems despite rotor resistance uncertainty," Automatica, vol. 32, no. 8, pp. 1127-1143, 1996.

[17] R. Datta and V. Ranganathan, "A simple position-sensorless algorithm for rotor-side field-oriented-control of wound rotor induction machine," IEEE. Trans. Ind. Elect., vol. 48, no. 4, pp. 786-793, Aug. 2001.

[18] R. Pena, J. Clare, and G. Asher, "Doubly fed induction generator using back to back PWM converters and its application to variable-speed wind-energy generation," IEE Proc. Electr. Power Appl., vol. 143, no. 3, pp. 231-241, May 1996.

[19] R. Marino, S. Peresada, and P. Valigi, "Adaptive input-output linearizing control of induction motors," IEEE Trans. Automat. Contr., vol. 38, no. 2, pp. 208-221, Feb. 1993.

[20] R. Marino, S. Peresada and P. Tomei, "Global adaptive output feedback control of induction motors with uncertain rotor resistance," IEEE Trans. Automat. Contr., vol. 44, pp. 967-983, May 1999.

[21] K. Gopakumar, V. Ranganathan, and S. Bhat, "Vector control of induction motor with split phase stator windings," Conf. Rec. IEEE-IAS Annu. Meeting, Denver, CO., pp. 569-574, Oct. 1994.

[22] R. Datta and V. Ranganathan, "Variable-speed wind power generation using doubly fed wound rotor induction machine—a comparison with alternative schemes," IEEE Trans. Energy Conv., vol. 17, no. 3, pp. 414-421, Sept. 2002.

[23] R. Datta and V. Ranganathan, "Direct Power control of grid-connected wound rotor induction machine without rotor position sensors," IEEE Trans. Power Elec., vol. 16, no. 3, pp. 390-399, May 2001.

[24] P. Krause, Analysis of Electrical Machinery. New York: McGraw Hill, 1986.

[25] E. Iyasere, M. Salah, E. Tatlicioglu, J. Wagner and D. M. Dawson, "Nonlinear robust control to maximize energy capture in a variable speed wind turbine using an induction generator," Clemson University CRB, Tech. Rep. CU/CRB/4/09/09/1, Apr. 2009. [Online]. Available: http://www.ces.clemson.edu/ece/crb/publictn/tr.htm

[26] G. Reklaitis, A. Ravindran, and K. Ragsdell, Engineering Optimization, Hoboken, NJ: John Wiley & Sons, 1983, pp. 41-130.